RICE UNIVERSITY

NMR MEASUREMENT OF DIFFUSION IN LIQUIDS BY THE PULSED FIELD GRADIENT TECHNIQUE

by

THOMAS F. EGAN

A THESIS SUBMITTED
IN PARTIAL FULFILLMENT OF THE
REQUIREMENTS FOR THE DEGREE

MASTER OF ARTS

APPROVED, THESIS COMMITTEE:

Harold E. Rorschach
Harold E. Rorschach
Professor, Physics
Chairman

James P. Hannon
Professor, Physics

Thomas L. Estle
Professor, Physics

HOUSTON, TEXAS

JANUARY, 1983

ABSTRACT

NMR MEASUREMENT OF DIFFUSION IN LIQUIDS
BY THE PULSED FIELD GRADIENT TECHNIQUE

by

THOMAS F. EGAN

The diffusion coefficient is an important parameter for characterizing the state of water in biological systems. A nuclear magnetic resonance method of diffusion measurement by the pulsed field gradient technique is described. A 90-τ-180 spin-echo sequence is used with one gradient pulse located on each side of the 180 rf pulse. Information on restricted diffusion is obtained by varying the measuring time, which is determined by the separation of the gradient pulse pair. Measuring times greater than 2 msec are possible with the present apparatus. Maximum magnetic field gradients of 110 gauss/cm are applied to cylindrical sample volumes of 1 cm diameter and 0.5 cm in height. This permits the measurement of diffusion coefficients as low as 10^{-7} cm^2/sec.

Details of the electronic hardware and gradient coil construction and calibration are given. The measurement process is software supported and includes digital data acquisition.

ACKNOWLEDGEMENTS

I would like to thank Professor H.E. Rorschach for his guidance in this research, and Professors J.P. Hannon and T.L. Estle for serving on the thesis commitee.

I also thank co-workers D. Bearden, D. Heidorn, and E.C. Trantham for their assistance in the laboratory.

Finally, I thank S. Preston for his technical support in preparing this manuscript.

TABLE OF CONTENTS

INTRODUCTION

The significance of water in biological systems is well recognized. A detailed understanding of water in the cellular environment is essential to explain transport properties, membrane permeabilities, and on some scale, all dynamical processes of the cell. Many studies have confirmed that cellular water differs in its properties from pure bulk water. Characterizing these differences on a microscopic physical basis is the subject of on-going research.

Apart from the problem of cell-associated water, a correct microscopic theory of bulk water remains unsolved. Cooperative effects due to hydrogen bonding in water have been approximated by cluster calculations with limited success (1). A generalized description of liquid water is given in terms of a competition between long-range ice-like ordering and structure-breaking exchange transitions by individual water molecules.

In biological systems, the state of water is altered by the complex structural composition of the cell and dilute ionic concentrations. The dipole moment of water is responsible for the formation of an 'hydration layer' around ions, at solid interfaces which may be polarizable, or at sites of fixed

charge. The distance over which this interaction is effective in modifying the properties of water is not well characterized. One model separates cell-associated water into two components: a 'bound' fraction local to the interface, and a larger 'free' fraction displaying bulk water properties for the remaining intracellular water (2). The water adsorbed to solid surfaces is assumed to extend only to the first few molecular layers. In this picture, 'bound' and 'free' water molecules are in rapid exchange, and this prevents classifying cellular water as two distinct non - interacting phases.

There is no general agreement on the extent of long range ordering of interfacial water. The compactness of structure in the cell is known to result in large surface area to volume ratios for the intracellular space. Under these conditions, water is in close proximity to multiple surfaces where ordering forces may influence its properties. This situation has prompted the development of models that include a pervasive reorganization of water throughout the cell (3).

The crucial question asked when dealing with physical measurements on biological systems is: are the measurements relevant to the living state? The interrelationship of water to cell structures is critical to biological functions. Two widely used non-ionizing physical probes of intact biological specimens are nuclear magnetic resonance and quasi-elastic neutron scattering. Pulsed NMR measurements of the diffusion coefficient for cellular water show a reduced value compared to bulk water (4). Neutron scattering results also suggest a structuring of cell-associated water greater than that of bulk water. Interpretation of all data is hindered by the complexity of the cell, but studies of simpler model polymer systems, among them: poly(ethelene oxide) and agarose gel (5), have been of assistance.

The mobility of cellular water is also influenced by hydrodynamic forces associated with the structured environment of the cell. Except for geometrically simple configurations of idealized barriers and obstructions, exact solutions for general restricted diffusion problems are not known (6). Neutron scattering techniques are capable of studying diffusive properties over a distance on the order of angstroms and provide information on short range diffusion and oscillatory motion (7). Modern NMR diffusion measurements sample over a well-defined distance of the order of or greater than one micron (8). At intermediate distances a wide range of structure sizes contribute to affect the diffusive behavior of water. (This extensive region is, as yet, not easily accessable to research under biological conditions, although light scattering is applicable for some non-opaque systems.)

This work reports the development of the pulsed field gradient technique, an improved method of diffusion measurement due to Stejskal and Tanner (9) that has been adopted at the physics NMR laboratory at Rice University. The pulsed field gradient technique offers two important capabilities: first it extends the range of determining small diffusion coefficients, and secondly it permits the examination of certain restricted diffusion problems.

THEORY

NMR theory is developed extensively in several texts (10,11). The discussion of NMR theory presented in this section will focus on material pertinent to research conducted at the Rice NMR facility and especially to diffusion measurement techniques.

In a magnetic field, each energy level of a spin 1/2 particle will split into two levels with separation ΔE. Transitions between levels are induced by absorption or emission of energy at the resonance condition:

$$E = \hbar w = \hbar \gamma H$$

where γ is the gyromagnetic ratio and H is the magnitude of the magnetic field. A proton is a spin 1/2 particle with $\gamma = 2.675 \times 10^4$ rad/gauss-sec. A non-zero nuclear spin implies a nuclear magnetic moment given by:

$$\vec{u} = \gamma \vec{L} = \gamma \hbar \vec{I}$$

Components of the magnetic moment perpendicular to the static field $\vec{H}$ (usually taken in the z-direction: $\vec{H} = H \hat{z}$) oscillate in time at w, the Larmor frequency.

Classically the magnetic field will exert a torque on the magnetic moment:

$$\vec{T} = d\vec{L}/dt = \vec{u} \times \vec{H} \text{ ,or } d\vec{u}/dt = \gamma(\vec{u} \times \vec{H})$$

It is convenient to view this in a rotating coordinate system through the operator transformation:

$$d/dt_{fixed} = d/dt_{rotating} + \vec{W} \times \quad .$$

Then,

$$\vec{du}/dt_{rot} = \vec{u} \times (\gamma\vec{H} + \vec{W}) = \vec{u} \times \vec{H}_{effective} .$$

For $\vec{W} = -\gamma\vec{H}$, $\vec{u}$ is stationary in the rotating frame, ie. $\vec{u}$ precesses at the Larmour frequency, $w = \gamma H$, in the laboratory frame about the z-axis. The magnetic moment per unit volume averaged over a macroscopic volume is defined as the magnetization, $\vec{M}$.

The addition of a second external magnetic field, $\vec{H}_1$, along the x-axis of the rotating coordinate system (let x',y',z' be coordinates in the rotating frame) at resonance will give $\vec{H} = H_1 \hat{x}$. In the rotating frame $\vec{M}$ will precess about $\vec{H}_1$, ie. in the y'-z' plane. Application of H_1 in a pulse of width Δt will reorient $\vec{M}$ through an angle $\Theta = \gamma H_1 \Delta t$. For a spin system initially in equilibrium with $\vec{M}$ along z, a 90° pulse will rotate $\vec{M}$ by 90° onto the y'-axis. Such a non-equilibrium distribution of spins (in the liquid state) will decay by relaxation mechanisms according to the Bloch equations:

$$d\vec{M}/dt = \gamma(\vec{M} \times \vec{H}) - (M_x\hat{x} + M_y\hat{y})/T_2 + [(M_o - M_z)/T_1]\,\hat{z}$$

where M_o is the equilibrium magnetization. T_1 is termed the spin - lattice or longitudinal relaxation time and T_2 is the spin - spin or transverse relaxation time.

Consider a net magnetization in the x-y plane (e.g. as prepared by a 90° pulse). Any variation in H, ΔH, will produce a distribution of resonant frequencies within the spin system of $\Delta w = \gamma \Delta H$. With respect to the rotating frame, the spins will begin to dephase during free precession (free induction decay). Sources of field inhomogeneity are two - fold: those of microscopic origin causing local field fluctuations, such as those due to dipole - dipole interactions responsible for irreversible T_2 processes, and

inhomogeneity in the applied external magnetic field. A 180° rf pulse at $t=\tau$ will cause the spin system to 're-focus' at $t=2\tau$ where a spin-echo will appear as in fig. 1 (12), with a smaller amplitude than for free induction decay since complete phase coherence of spins is not maintained because of T_2 processes. Allowing for motional freedom, translational diffusion by individual spins will also result in permanent loss of phase coherence.

NMR measurements of translational diffusion rely upon an externally imposed spatially - dependent magnetic field to 'label' the nuclear spins. For example, a magnetic field gradient in the z-direction will establish a phase relationship between any two spins that depends upon their separation along the z-axis. Diffusional motion occuring in the spin system as well as T_2 processes will thus produce a reduced echo amplitude in the 90-τ-180 sequence spin-echo experiment.

The modification of the Bloch equations to include diffusion is due to Torrey (13). The additional term is of the form:

$$\vec{dM}/dt = D\nabla^2\vec{M} ,$$

where D is the diffusion coefficient. Solutions to the Bloch - Torrey equations for specific time-dependent applied field gradients have been developed and experimentally verified by Stejskal and Tanner (9) for the spin-echo technique. Their treatment of this problem is summarized in an appendix.

Early NMR diffusion measurements on liquids by field gradient methods were done with a constant gradient, G_o . The echo amplitude reduction is:

$$\ln(A/A_o) = - D(2G_o^2\tau^3)/3 .$$

In principle G_o could be made arbitrarily large to offset small D values; however, the magnetic moment frequency distribution is proportional to G_o :

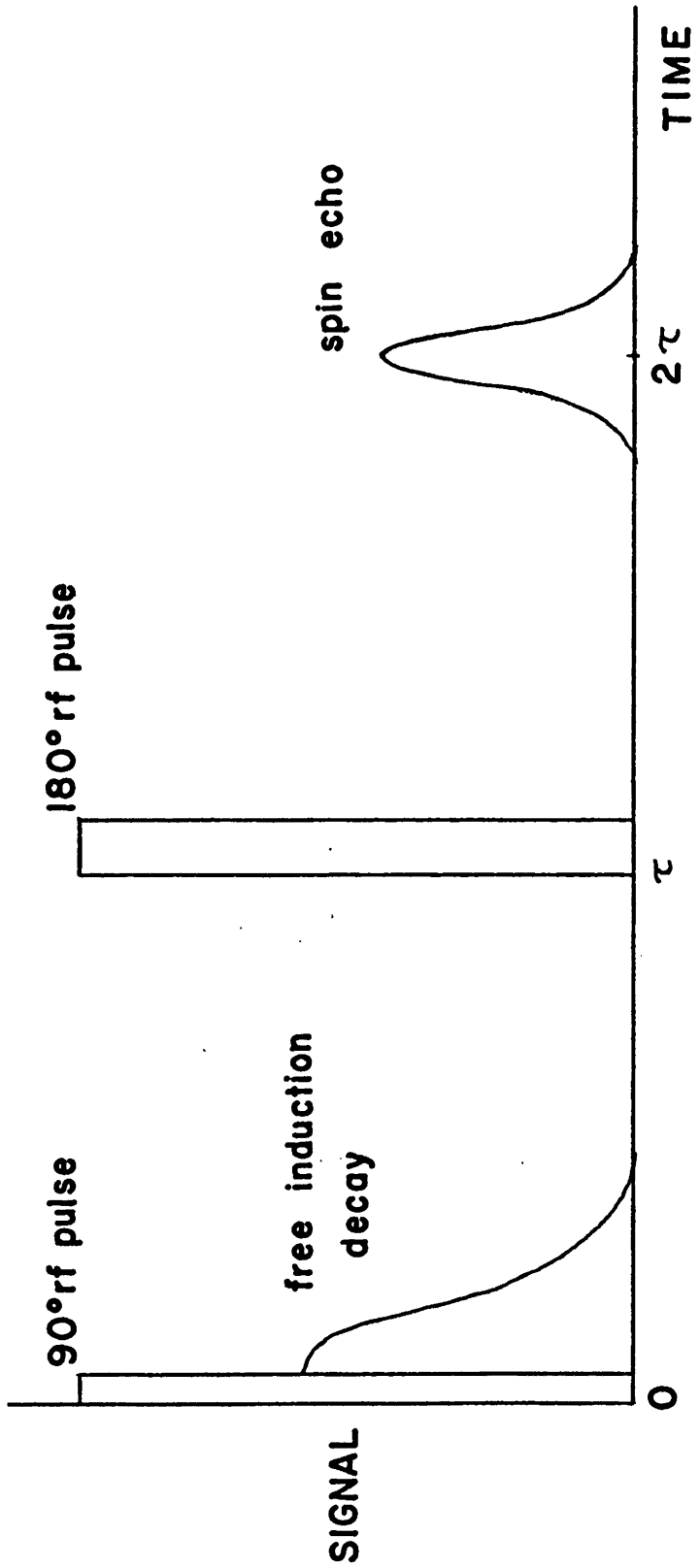
SIGNAL
90°rf pulse
free induction
decay
180°rf pulse
spin echo
0
τ
2τ
TIME

FIGURE 1

$$\Delta w = \gamma \Delta H = \gamma G_o \Delta z$$

for a gradient in the z-direction. The spread in frequencies corresponds to a narrowing of the echo in the time domain, and is a limiting factor on the magnitude of G_o . Aside from hardware design considerations, further technical problems concern the detrimental effects of strong steady gradient fields located at the sample during rf excitation: conditions for uniform 90° rotations and 180° inversions of $\vec{M}$ over the sample volume can not be met.

In most applications of the pulsed field gradient technique, $G \gg G_o$; G_o is the residual constant gradient. For this situation:

$$\ln(A/A_o) = -D(\gamma \delta G)^2(\Delta - \delta/3) .$$

PFG techniques are effective from the standpoint of delivering high field gradients at the sample (order of magnitude larger than constant gradient) without signal degradation caused by detection bandwidth limitations. Pulsed gradient methods also place less stringent demands upon the power - handling capabilities of the gradient field coils and associated electronics. However compared to the constant gradient method, provisions for switching large current pulses require a substantial increase in electronic sophistication.

The diffusion time Δ (for $\Delta \gg \delta/3$) is well-defined in PFG experiments and independent of τ , provided that $G \gg G_o$. The spin-echo at $t=2\tau$ can be optimally positioned while retaining the flexibility of a variable diffusion time.

In studies of restricted diffusion, one approach is to measure the diffusion coefficient as a function of diffusion time. The rms diffusional distance moved in a time t is:

$$d = (2Dt)^{1/2} .$$

Information on structural dimensions in biological systems is obtained by

examination of effective diffusion coefficients of cellular water as a function of measuring time Δ; ie. the ratio of the measured D to the bulk water value D_o. Variation of D/D_o with Δ is an indication of barriers and/or obstructions to diffusion.

Restricted diffusion and multiple-component mixtures with differing diffusion rates will show-up as deviations from the predicted exponential behavior. Some theoretical progress in diffusion boundary-value problems has been made. Stejskal and Tanner (6) have determined expressions for diffusion in stacked impermeable planar barriers and spherical compartments. Rorschach and Hazlewood (14) estimate effective diffusion coefficient corrections for diffusion through an ordered array of obstacles. Close analogues of these model systems exist in the biological environment, such as membrane barriers, and some tissue superstructures such as fiber networks in muscle (14). Both numerical and approximate analytical solutions to bounded medium NMR diffusion problems are discussed by Wayne and Cotts (15) and Robertson (16). Neuman (17) has extended the calculation of restricted diffusion effects to include planar, spherical, and cylindrical boundaries.

EXPERIMENTAL METHODS

NMR

The hardware and electronic requirements for pulsed NMR experimentation have been described in detail elsewhere (10). The Rice University physics dept. NMR laboratory is equipped with a Bruker superconducting magnet and Bruker SXP spectrometer. A stable radio frequency source (General Radio 1165 frequency synthesizer) is gated by the programmable pulse generator. The modulated radio-frequency burst is amplified and transmitted to the sample at the Bruker probe head. The resonance signal is detected through the wide-band probe head and preamplified. Final amplification takes place at the spectrometer receiver where both phase sensitive and diode detection are available.

Proton magnetic resonance is observed at 30 Mhz in an external magnetic field of 7.2 kGauss. Spin echo data is displayed on a Nicolet 1074 digital storage oscilloscope. An Interdata 7/16 computer system provides data processing.

PFG coils

Following the design parameters reported by Tanner (18), a gradient coil was constructed (by E.C. Trantham and G. Gist) to give optimal gradient uniformity. Two magnetically opposed Helmholtz coils, 4 turns each, were wound with no. 28 gauge wire around a recessed channel cut into a cylindrical teflon rod. The diameter of each coil is about 1.49 cm and the

coils are separated by 1.41 cm. The teflon cylinder was bored to accept a ten millimeter sample test tube. The outside diameter of the teflon former was chosen to fit snugly into a 20 mm test tube which in turn fits into the probe head. Electrical resistance of the coils is 0.6 ohms.

With the gradient coil assembly in place, the axis of the coils is along the external field. Then the calculated gradient along the z-axis, if the wires are treated as lines of current, is:

$$G \simeq dH/dz_{z=0} = -2\pi INa^2(d/2c)\left[a^2 + (d/2)^2\right]^{-5/2}$$

where a is the coil radius, d is the coil separation, I is the current, and N is the number of turns, all in cgs units. The plane at z=0 is midway between the coils. For the dimensions stated: G/I = 5.18 gauss/cm-Amp, current in mks units. The normal sample height is 0.5 cm centered about z=0. The absence of magnet pole faces or magnetic materials near the gradient coils eliminates eddy current pertubations of the gradient field.

Carr and Purcell (19) have discuussed a method for calibrating the gradient field utilizing a constant gradient technique. Following a 90° rf pulse, the $M_{y'}$ distribution function is given in the notation of Carr and Purcell by:

$$M_{y'} = M_o \int f(H_z) \cos\left[\gamma(H_z - H_{zo})t\right] dH_z ,$$

where $f(H_z)dH_z$ is the fraction of nuclear spins located in a field of H_z. The field H_z represents the contributions from both microscopic and external sources. An applied constant field gradient over the sample volume can be made to dominate other sources of field inhomogeneity so that $H_z = H_{zo} + Gz$. For a cylindrical sample volume, axis along z, with area A and height h,

$$M_{y'} \simeq M_o/Ah \int_{-\frac{h}{2}}^{\frac{h}{2}} A\, dz \cos(\gamma Gzt) .$$

Then:

$$M_{y'} \simeq \sin(\gamma G(h/2)t)/\gamma G(h/2)t \ .$$

The first zero of the distribution is for:

$$G(h/2)t_o = \pi \ .$$

Since the distribution is symmetric if the spin-echo following the 180° rf pulse is observed, $\Delta t=2t_o$ is the time interval between the zeroes of the distribution around the central peak, and

$$G = 4\pi/\gamma \Delta t \ h \ , \text{ so that}$$

$$G/I \ \gamma h/4\pi \ \Delta t = I^{-1} \ .$$

A plot of I^{-1} vs Δt is shown in fig. 2. From a least squares determination of the slope, G/I = 5.08 gauss/cm-A; which agrees well with the calculated value (Carr-Purcell quote an uncertainty on the order of 5% for this procedure). A value of 5.1 gauss/cm-A was chosen for the gradient to current ratio in diffusion coefficient calculations.

PFG electronics

The basic PFG electronic hardware consists of a pulse-generator/timer and switching circuitry for current amplification. In most applications, millisecond capabilities are required for the pulse width and spacing parameters, and pulsed currents of 10 - 20 Amps or more are required. In the original design by Tanner (18), a series of automobile-type batteries served as the power supply, and transistor switching was introduced. The PFG switching circuit constructed and now in operation is a modified version of the design by Callaghan et al. (20).

A schematic of the high current switching electronics is shown in fig. 3. The design includes an optical isolator (TIL 111) at the input stage, and the three transistors are configured in a darlington arrangement. The resistors R_v and R_p in series with the gradient coils are non-inductive types. The power

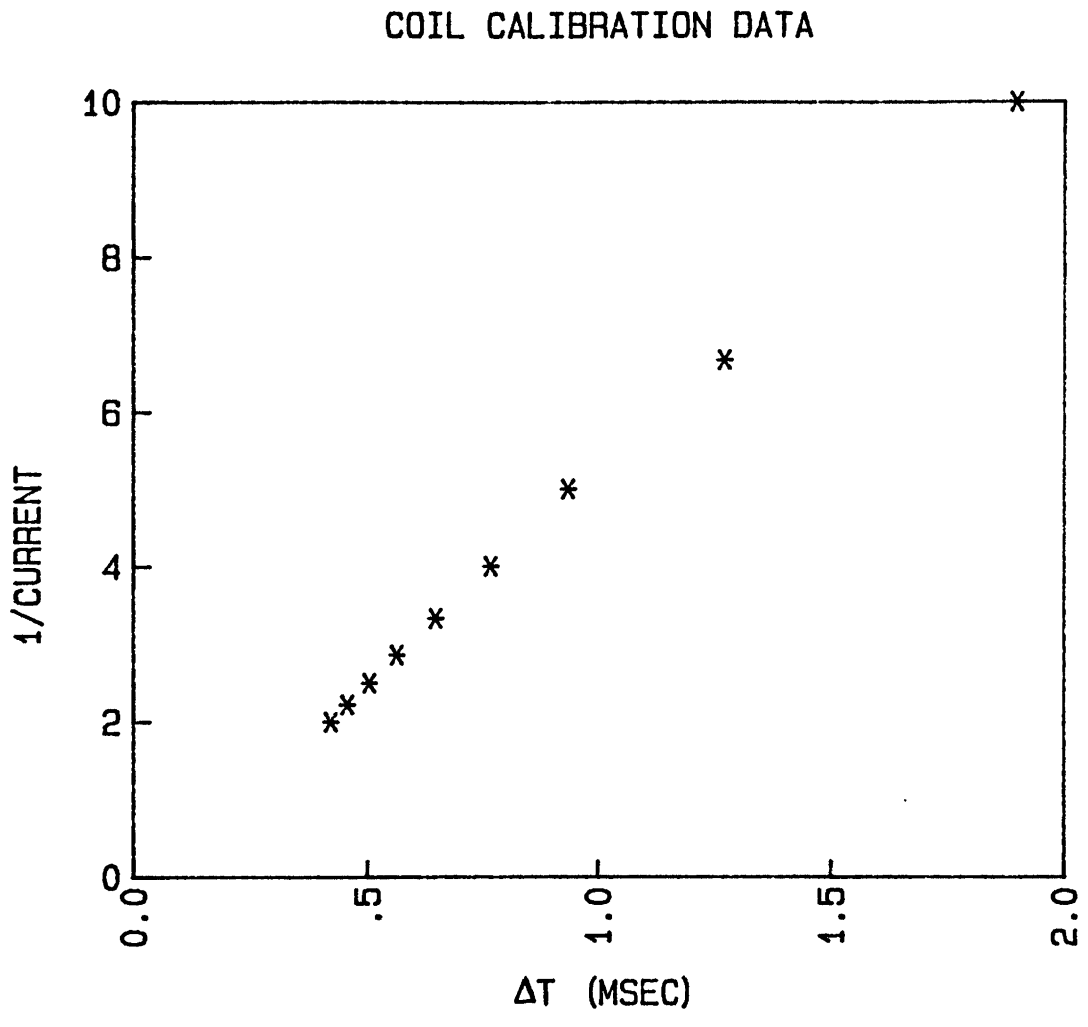

FIGURE 2

supply is four 12V heavy-duty batteries which give an output of +24V, +12V, and +19V thru a 7905 voltage regulator (see fig. 4). The current is determined by a differential amplifier connected across the presision 0.1 ohm resistor R_p (built by D. Bearden) as shown in fig. 5.

Pulse inputs to the switching electronics are obtained from the spectrometer pulse programmer. Four outputs are available from the programmer: A,B,C, and D. Output pulses A and C are used for the 90 and 180 rf pulses, and B and D for the gradient pulses so that in a spin-echo experiment, the pulses A thru D are sequential. The time delay of each pulse is adjustable and referenced from the preceeding one. The amplitudes of the B and D pulses are 5.5V into 50 ohms with rise and fall times of 20 and 15 nsec respectively. All input/output connections are BNC-type cable.

Gradient pulses of 1 msec width have rise and fall times of 20 microseconds or less up to the maximum current of about 20 Amps. Sag is less than 2%. The differential amplifier was calibrated with an input of known current; the response is linear over the operating range. Residual DC current leakage is zero to within the noise limits of the differential amplifier or by direct measurement with a digital multimeter.

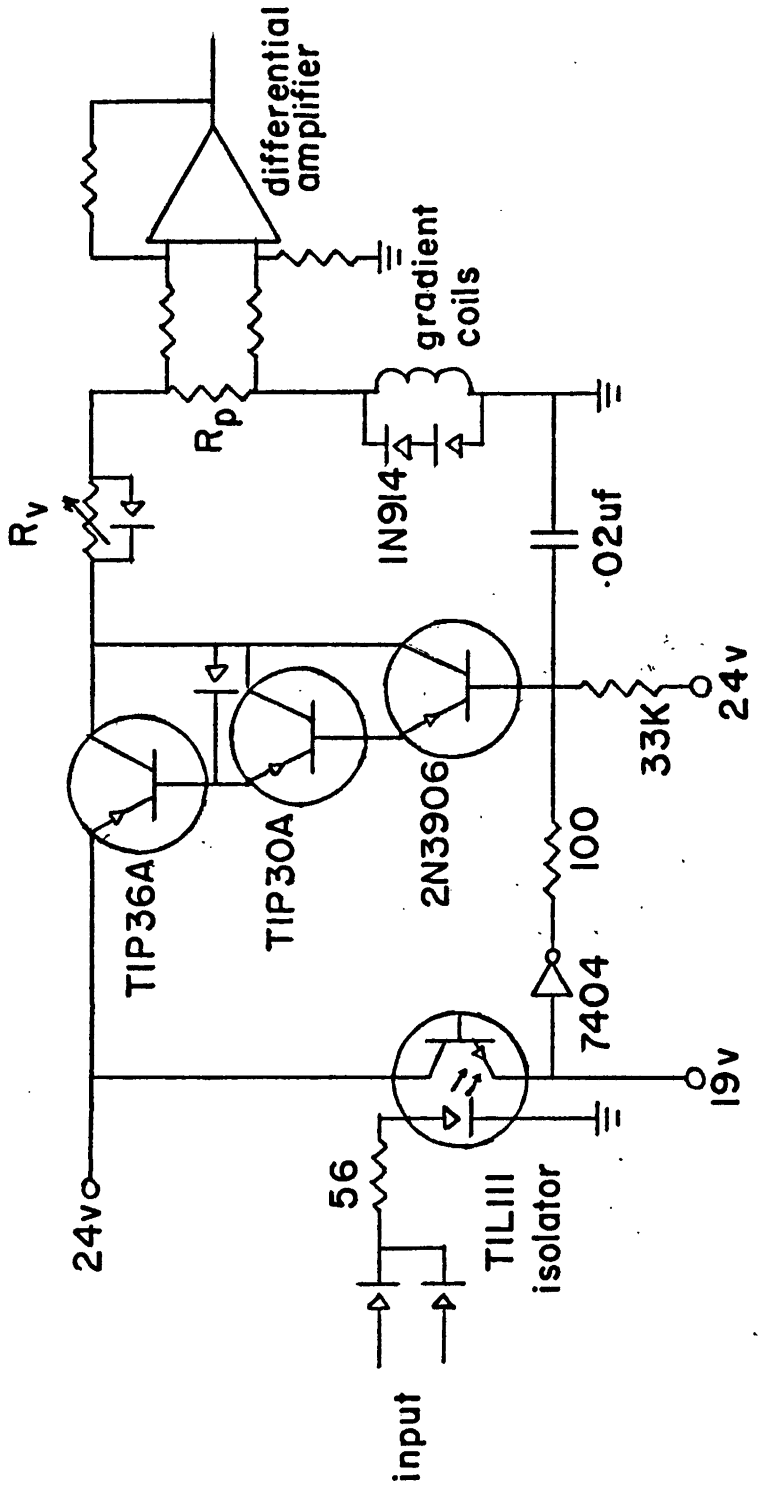
differential amplifier
gradient coils
R_p
R_v
IN914
.02uf
TIP36A
TIP30A
2N3906
33K
24v
100
7404
19v
24vo
56
TIL111 isolator
input

FIGURE 3

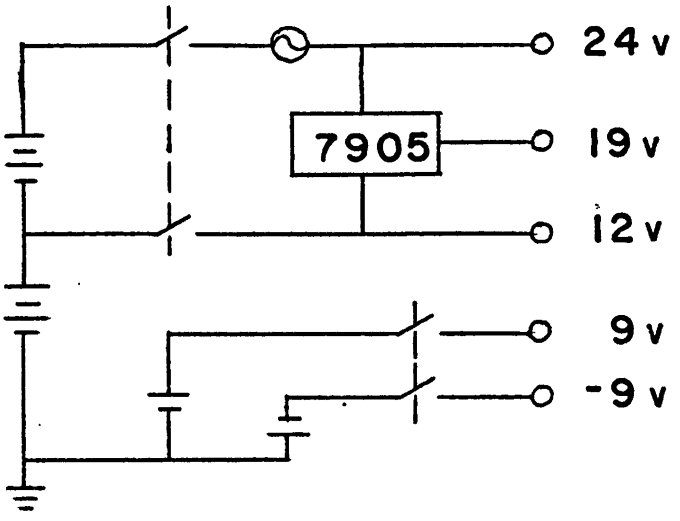

FIGURE 4

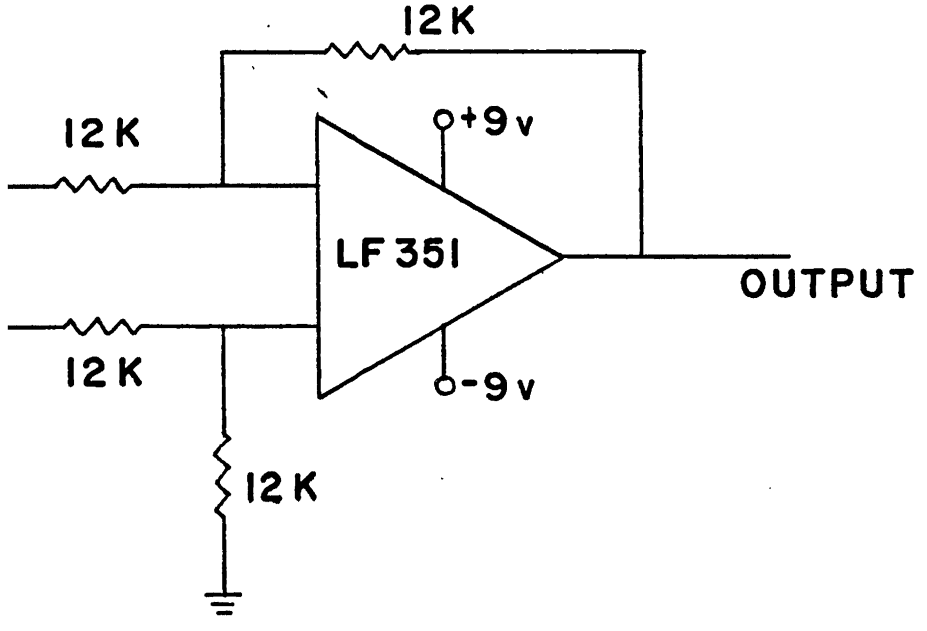

FIGURE 5

OPERATING PROCEDURE

Diffusion data acquisition and analysis has been automated to a large degree through the Interdata 7/16 computer system and Nicolet 1074 digital oscilloscope. Existing software developed by E.C. Trantham for NMR relaxation measurements was modified for use in PFG diffusion measurements by D. Bearden.

Initially, a well - tuned $90\text{-}\tau\text{-}180$ pulse sequence is established with observation of a spin-echo at 2τ. The gradient pulse width, δ, is manually set on the pulse-programmer control panel (pulses B and D). Pulse time delays are set such that the time between A and C pulses is τ and that between B and D pulses is Δ, with $\Delta < 2\tau$.

Computer control of the measurement process is directed in real time at the Intertec terminal. In this interactive operating mode, the temporal positioning of maximum echo amplitude is verified to be at the 2τ location on the Nicolet as designated by a computer calculation. The criterion used to equalize the two gradient pulse widths is formation of a symmetric echo with a peak at 2τ. Fine adjustment of one of the gradient pulse widths is performed while slowly increasing the gradient field strength until the echo remains approximately centered at 2τ for the highest gradient field for which the echo is still detected. The nominal values of δ and Δ are entered at the terminal for later use in a more precise determination.

The gradient field strength depends on the value chosen for the variable

resistor R_v ; the resistance range is 0.1 to 99.9 ohms. A small gradient field on the order of 30gauss/cm (6 amps) is reached at an indicated value of 30 ohms.

After the tuning segment of the procedure and selection of a gradient field, one or more echos are manually collected on the Nicolet. Several echos are accumulated and averaged by the Nicolet; the specific number is conditional on signal strength. A command from the terminal then instructs the computer to read the Nicolet data buffer, and digital data is transferred for processing. Typically, the spin-echo signal is sampled at 10-30 usec/point resulting in a few hundred points describing the echo waveform. Echo height is computed by fitting a parabolic curve to the data points in a small region of time centered around 2τ (the software uses 40 points on each side of the 2τ height or steps out to 0.7 times the 2τ height, whichever is the smaller).

Immediately on completion of echo height processing, a relay is opened which switches the signal monitored by the Nicolet from the spectrometer receiver to the differential amplifier of the PFG electronics. The two voltage pulses are displayed on the Nicolet under identical conditions for which the spin-echo was observed . An estimation based on this digital data is made for the pulse width and separation. The pulse amplitude is converted to a current scale. The relay is automatically closed and the data collection process is reinitialized and may be repeated for either the same or a different gradient field.

Echo heights for at least ten different gradient fields are collected for a particular diffusion measurement. The A_o amplitude is measured with the variable resistance set to maximum, 100ohms, and gradient pulses still operating. It was found that this amplitude was the same or slightly greater

than that with the PFG electronics off. Also, the experimental consistency is improved if a steady-state pulsing sequence is maintained due to better pulse width stability.

RESULTS

The analysis of PFG diffusion data under conditions where $G \gg G_o$ is by

$$\ln(A/A_o) = -D(\gamma \delta G)^2(\Delta - \delta/3) .$$

The magnetic field gradient G is the product of the coil calibration constant, 5.1 gauss/cm-A, and the current thru the coil in Amps. For fixed Δ and δ, a semi-log plot of echo attenuation versus current squared is linear for homogeneous unbounded systems characterized by a single diffusion constant. Departure from the single exponential form for echo amplitude vs. $G^2 \delta^2(\Delta - \delta/3)$ suggests the presence of barriers and obstructions to diffusion or multiple component diffusion.

Testing of the PFG hardware and electronics was completed with proton magnetic resonance observations on pure water, 5 millimolar FeCl -doped water, and water/glycerin mixtures. In all cases, the sample height was about 0.5cm. The result of one diffusion measurement for pure water is shown in fig. 6; with δ=1msec, Δ=10msec, and τ=20msec (each point is the average of four consecutive spin-echo sequences with a repetition rate of 10 seconds). An exponential fitting routine using the Marquardt algorithm was used to determine the diffusion coefficient, yielding $D=1.94 \times 10^{-5}$ cm^2/sec. A second data set is shown in fig. 7, but with δ=0.5msec, $\Delta = \tau$=30msec, and $D=2.14 \times 10^{-5}$ cm^2/sec.

The uncertainty in the fitting parameters is small, less than 1%, and indicates the data do conform to the predicted single exponential behavior.

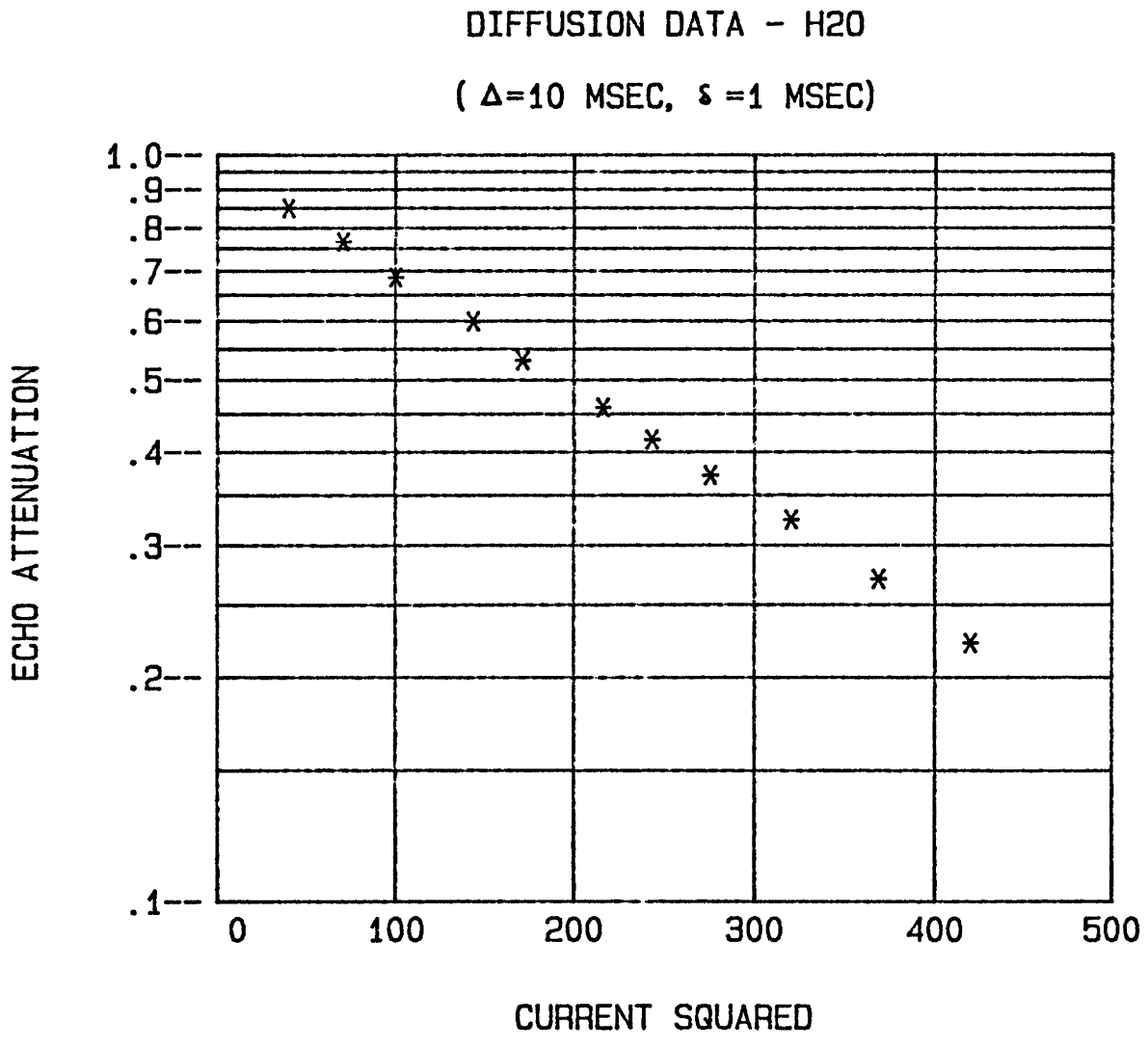
DIFFUSION DATA - H2O
(Δ=10 MSEC, δ =1 MSEC)
ECHO ATTENUATION
1.0--
.9--
.8--
.7--
.6--
.5--
.4--
.3--
.2--
.1--
0
100
200
300
400
500
CURRENT SQUARED

FIGURE 6

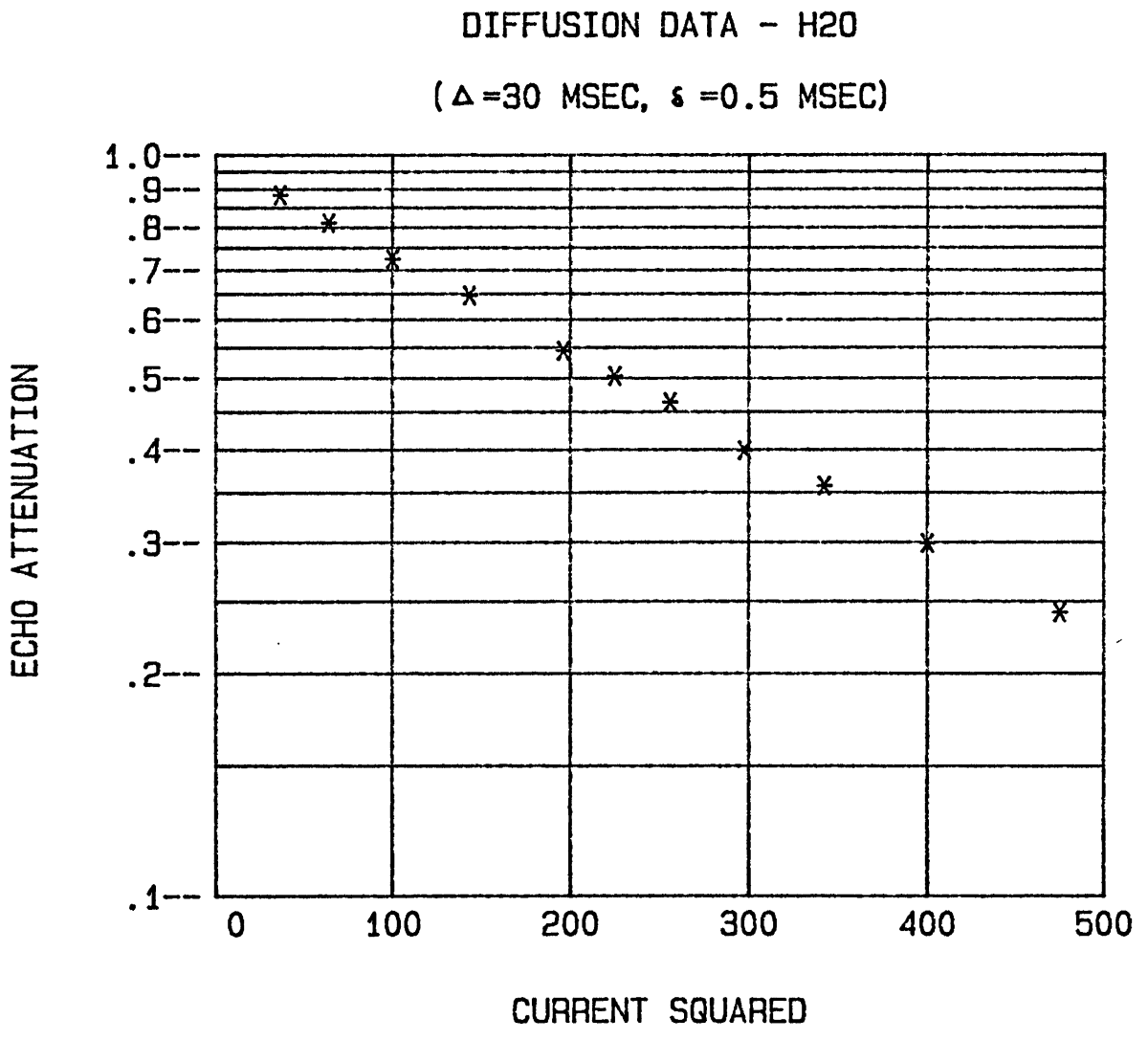
DIFFUSION DATA - H2O
(Δ=30 MSEC, δ=0.5 MSEC)
ECHO ATTENUATION
1.0
.9
.8
.7
.6
.5
.4
.3
.2
.1
0
100
200
300
400
500
CURRENT SQUARED

FIGURE 7

Direct numerical comparisons of these data with diffusion coefficients reported by other laboratories is complicated by the temperature dependence of diffusion rates and non-standardization of water purity. Diffusion measurements on water have mainly been of two types: by NMR techniques and by tracer methods with most findings lying in the range of 2.3 - 2.5×10^{-5} cm^2/sec at 25 C (21). Tanner (8) obtains a value of $D=2.3 \times 10^{-5}$ cm^2/sec for pure water at a temperature of 27±2 C by the PFG technique.

The diffusion coefficient depends upon the temperature through an Arrhenius relationship:

$$D = D_o \exp(-E_a/kT)$$

where E_a is the activation energy. Temperatures of liquid samples in the magnet bore have been observed to vary between 15 C and 25 C over the course of 2-3 months of testing. The exact temperature of the data shown in figs. 6 and 7 is not known, however 20±2 C is a rough estimate. Extrapolation of Tanner's reported diffusion coefficient to 20 C gives $D=1.9 \times 10^{-5}$ cm^2/sec (for an activation energy of 4.6 kcal/mole from reference 21).

In this research, diffusion measurements on both pure water and the doped-water preparation covered a range of values from 1.8 - 2.5×10^{-5} cm^2/sec. The large variation is thought to be temperature induced as the distribution was strongly correlated with temperature. Immediate repetitive measurements, with constant δ and Δ, on a sample resulted in highly reproducible diffusion coefficients. Total measurement time is on the order of 10 - 15 minutes and sample temperature drifts are small in this time.

A 50% by volume mixture of glycerin and water was prepared and the diffusion coefficient was determined to be 4.5×10^{-6} cm^2/sec. This compares well with data obtained by Seitz (22) for constant gradient diffusion measurements on water/glycerol mixtures.

The good single exponential fits to the PFG diffusion data in figs. 6 and 7 suggest that the main experimental uncertainty resides in the pulse parameters δ and Δ, and the gradient field G. For δ =1msec, the estimated error for a single pulse width determination is 5%; however an average over at least ten independent measurements of δ is used in the diffusion coefficient calculation. Error in the measured Δ is less than 1% for Δ>10msec. Initially the field gradient calibration is probably not known to better than 5%; however repeated close agreement of diffusion coefficients to accepted values is reason to believe a lower estimate is appropriate. Errors in current determination are negligible in comparison with other errors mentioned above. The net estimated uncertainty for a single diffusion measurement, and $D \sim 10^{-5}$ cm^2/sec, is 5-10% for $\delta \sim 1$ msec and $\Delta \sim 10$msec.

For systems with small diffusion coefficients, relatively large pulse widths are required to produce comparable echo attenuation. The upper bound on δ is τ; however stable echoes have been produced only with δ up to 4-5 msec due to lack of adequate fine adjustment control of the pulse width, which is critical to echo formation. The electronic limitations will result in smaller differences in echo amplitudes and therefore smaller slopes for plots as in figs. 6 and 7. The random error in echo amplitude is more significant in these circumstances and may be suppressed by averaging more echos with the uncertainty being diminished by the factor $1/\sqrt{n}$ for n measurements.

CONCLUSION

The measurement of small diffusion coefficients requires the application of gradient pulses of large area (field strength x time). The maximum gradient possible with the present apparatus is 110 gauss/cm. Pulse widths up to 4 msec have produced stable spin-echos. This combination gives a lower limit for reliable measurement of diffusion coefficients of 10^{-7} cm^2/sec.

In systems exhibiting restricted diffusion, the effects of barriers and obstructions can be observed by varying the measuring time Δ (or $\Delta - \delta/3$ for $\delta \sim \Delta$). The smallest pulse separation now possible is 2 msec (assuming δ is <1 msec). Since the echo attenuation is proportional to δ^2 and Δ, higher gradient fields are required to produce comparable spin-echo amplitudes for short measuring times. If larger fields are not available, then the accuracy of diffusion coefficient determination may be impaired.

One approach to assist diffusion measurement in the small measuring time region is another gradient pulse sequence developed by Tanner (8). The sequence consists of a train of N alternating sign gradient pulse pairs applied between the time 0 and τ followed by N pairs between τ and 2τ . In the absence of a constant gradient field, the echo attenuation is given by:

$$\ln(A/A_0) = -2ND(\gamma \delta G)^2(\Delta - \delta/3) .$$

The time Δ is the constant time interval between succesive leading edges of the positive and negative gradient pulse pair. With the alternating sign

configuration, measuring times as low as 0.4 msec have been obtained by Tanner corresponding to a rms diffusion distance of ~1 micron for water.

For the two-pulse field gradient technique currently in operation, ie. one positive pulse on either side of τ , N=1/2. Revision of the existing pulsing circuitry to accommodate the alternating sign configuration is being planned. In addition to providing benefits at small measuring times, this modification should extend the lower limit of reliable diffusion coefficient measurements.

A second improvement in terms of obtaining consistent diffusion data is the installation of a temperature control system. Provisions for a heater unit and temperature sensor have been incorporated at the sample holder in the Bruker probe head. Temperature regulation will be provided by a YSI model 729 proportional temperature control (see Cleveland(23)) to an accuracy of a few tenths of degrees C.

A newly acquired Nicolet 4094-2 digital oscilloscope will improve the diffusion data acquisition process. This instrument features a temporal resolution 10 times greater than the Nicolet 1074 it replaces. The dual-channel input capability will provide for the spin-echo and current pulse data to be monitored coincidently. The 4094 is interfaced to the Interdata 7/16 computer, and digital data may be either read from or written to the instrument and displayed.

Also under consideration are plans for upgrading the performance and interface capability of the spectrometer pulse generators. This is part of the effort to automate further the PFG data collection process.

In order to evaluate the potential for restricted diffusion studies on biological materials, two model systems are under study: a glass capillary array manufactured by Gallileo Optics, and poly(ethylene-oxide)-water

solutions. The microchannel plate is a glass wafer 2mm thick and 8mm in diameter consisting of a bundle of highly uniform 5 micron diameter close-packed channels extending the full 2mm depth. The capillaries are filled with water, and diffusion measurements performed with the cylinder axis parallel and perpendicular to the gradient field. Preliminary results show an anisotropy in the diffusion coefficient for measuring times in the range of times corresponding to the known barrier dimensions, with the parallel diffusion greater than that of the perpendicular orientation by a factor of 4, but smaller than the bulk water value.

Extensive research of proton diffusion dependence on hydration for poly-ox/water solutions has been completed by D. Bearden (24). These data have been fit to various compartmental-effect theoretical models. Information on the size of these compartments may be obtained by diffusion measurements sensitive to the distance scales involved.

REFERENCES

1. A.T. Hagler, H.A. Scheraga, and G. Nemethy, in Annals of the New York Academy of Sciences 204, edited by C.F. Hazlewood, (New York Academy of Sciences, 1973) 51.

2. R. Cooke and R. Wein, in Annals of the New York Academy of Sciences 204, edited by C.F. Hazlewood, (New York Academy of Sciences, 1973) 197.

3. G.N. Ling, in "Cell-Associated Water", edited by W. Drost-Hansen and J.S. Clegg, (Academic Press, New York, 1979) 261.

4. C.F. Hazlewood, in "Cell-Associated Water", edited by W. Drost-Hansen and J.S. Clegg, (Academic Press, New York, 1979) 165.

5. E.C. Trantham, Doctor of Philosophy thesis, Rice University, (1981).

6. J.E. Tanner and E.O. Stejskal, J. of Chem. Phys. 49, 1768 (1968).

7. T. Springer,"Quasielastic Neutron Scattering for the Investigation of Diffusive Motions in Solids and Liquids", (Springer-Verlag, New York, 1972).

8. J.E. Tanner, Self-diffusion in Cells and Tissues, Office of Naval Research Report NWSC/CR/RDTR-6, Division of Medical and Dental Science, Arlington, Va. (1975).

9. E.O. Stejskal and J.E. Tanner, J. of Chem. Phys. 42, 288 (1965).

10. T.C. Farrar and E.D. Becker,"Pulse and Fourier Transform NMR", (Academic Press, New York, 1971).

11. C.P. Slichter,"Principles of Magnetic Resonance", (Springer-Verlag, New York, 1978).

12. E.L. Hahn, Phys. Rev. 80, 580 (1950).

13. H.C. Torrey, Phys. Rev. 104, 563 (1956).

14. H.E. Rorschach and C.F. Hazlewood, Self-diffusion of Water in Ordered Protein Systems, unpublished.

15. R.C. Wayne and R.M. Cotts, Phys. Rev. 151, 264 (1966).

16. B. Robertson, Phys. Rev. 151, 273 (1966).

17. C.H. Newman, J. of Chem. Phys. 60, 4508 (1974).

18. J.E. Tanner, Rev. of Sci. Inst. 36, 1086 (1965).

19. H.Y. Carr and E.M. Purcell, Phys. Rev. 94, 630 (1954).

20. P.T. Callaghan, C.M. Trotter, and K.W. Jolley, J. of Mag. Res. 37, 247 (1980).

21. H.R. Pruppacher, J. of Chem. Phys. 56, 101 (1972).

22. P.K. Seitz, Doctor of Philosophy thesis, University of Texas at Austin, (1977).

23. G. Cleveland, Master of Arts thesis, Rice University, (1973).

24. D. Bearden, Master of Arts thesis, Rice University, (1982).

APPENDIX

Following a 90° pulse, the transverse magnetization in the rotating frame is given by:

$$dM^+(r,t) = -i\,\gamma\,(H(r,t)-H_o)M^+ - M^+/T_2 + D\nabla^2 M^+ ,$$

where $M^+ = M_x + iM_y$. The magnetic field H(r,t) is taken in the z-direction with magnitude:

$$H(r,t) = H_o + \vec{\nabla}H \cdot \vec{r} = H_o + \vec{G} \cdot \vec{r} .$$

The field gradient $\vec{G}$ may be a function of time. In the presence of boundaries and barriers to diffusion, solutions must satisfy proper boundary conditions. Solutions are obtained here for the infinite sample approximation; where diffusional distances are much less than dimensions of any barriers to translational motion.

First with D=0, solutions are of the form:

$$M^+(r,t) = M_o \exp(-i\,\gamma\,\vec{r} \cdot \vec{F}(t) - t/T_2) ,$$

where

$$\vec{F}(t) = \int \vec{G}(t')dt' .$$

With the diffusion term:

$$M^+(r,t) = M_o \exp(-i\,\gamma\,\vec{r} \cdot \vec{F}(t) - t/T_2)\; A(t) ,$$

where A(t) is to be determined from substitution back into the original differential equation. The result is:

$$t<\tau \qquad 1/A\; dA/dt = -\gamma^2 D\; F^2(t)$$

$$t>\tau \qquad 1/A\; dA/dt = -\gamma^2 D\; \left[\vec{F}(t) - 2\vec{F}(\tau)\right]^2 .$$

For $t>\tau$, ie. following a 180° pulse, $\vec{F}(t)$ is replaced by $\vec{F}(t)-2\vec{F}(\tau)$. The effect of the 180° pulse is to change the sign of $\vec{G}$:

$$\begin{aligned}\int_0^t \vec{G}(t')dt' &= \int_0^\tau \vec{G}(t')dt' + \int_\tau^t (-\vec{G}(t'))dt' \\ &= \vec{F}(\tau) - \int_\tau^t \vec{G}(t')dt' - \int_0^\tau \vec{G}(t')dt' \\ &= 2\vec{F}(\tau) - \vec{F}(t) \ .\end{aligned}$$

At a time t, for $t>\tau$:

$$\ln(A/A_0) = -\gamma^2 D \left[\int_0^t F^2(t)dt - 4\vec{F}(\tau) \cdot \int_\tau^t \vec{F}(t)dt + 4F^2(\tau)(t-\tau) \right] .$$

The simplest configuration of the pulsed field gradient technique calls for two identical gradient pulses of width δ and separation Δ, one on either side of the 180° rf pulse. Then:

$$\vec{G}(t) = \begin{cases} \vec{G}_0 & 0<t<t_1 \\ \vec{G}_0 + \vec{G} & t_1<t<t_1+\delta \\ \vec{G}_0 & t_1+\delta<t<t_1+\Delta \\ \vec{G}_0 + \vec{G} & t_1+\Delta<t<t_1+\Delta+\delta \\ \vec{G}_0 & t_1+\Delta+\delta<t \end{cases}$$

The complex phase factor in the exponential disappears at $t=2\tau$ as the spin echo is formed. The echo attenuation due to diffusion is given by:

$$\ln(A/A_0) = -\gamma^2 D\left[2/3 G_0^2 \tau^3 + \delta^2 G^2(\Delta - \delta/3) - \vec{G}\cdot\vec{G}_0(-2\tau^2 + (t_1^2+t_2^2) + \delta(t_1+t_2) + 2/3\,\delta^2)\right] ,$$

where $t_2 = 2\tau - (t_1+\Delta+\delta)$.